Available online at www.sciencedirect.com

ScienceDirect

Proceedings of the Combustion Institute 35 (2015) 711–719

Proceedings of the Combustion Institute

www.elsevier.com/locate/proci

Determination of burning velocities from spherically expanding H_2/air flames

Emilien Varea [a,*], Joachim Beeckmann [a], Heinz Pitsch [a], Zheng Chen [b], Bruno Renou [c]

[a] *Institute for Combustion Technology, RWTH Aachen University, 52056 Aachen, Germany*
[b] *SKLTCS, Department of Mechanics and Engineering Science, College of Engineering, Peking University, Beijing 100871, China*
[c] *CORIA UMR 6614 CNRS, INSA de Rouen, 76801 Saint Etienne du Rouvray, France*

Available online 25 June 2014

Abstract

Laminar burning velocities of hydrogen/air mixtures can show discrepancies up to 30%, making chemical mechanism validation and improvement difficult. The source of uncertainties may come from different factors influencing at each processing and post-processing steps the final value. Considering a spherically expanding flame configuration, reflection on the accuracy of the formulations, used to derive the desired quantity, is proposed. Starting from the exact definition of the laminar burning velocity, two formulations – direct and indirect flame speeds formulations – are derived for spherical flames. Each single source of uncertainty involved in the formulations is pointed out. The emphasis is focused on a specific mixture at an equivalence ratio of 0.50, atmospheric pressure, and an initial temperature of 300 K. This point represents the best tradeoff between low ratio of flame velocity and recording sampling rate and the occurrence of cellular flames (Le < 1). An extensive experimental and numerical study (1D spherically expanding flames) of this mixture is carried out. As a result, the experimental laminar burning velocities determined by using the direct flame speed or the indirect flame speed formulae depict different values. However, when numerically determined, both formulae yield the same value. This paves the way to understand and identify the experimental error sources. Stretch and Lewis numbers effects (super-adiabatic temperatures) as well as radiation processes (burned gas motion) are studied. Nonetheless, they do not show to be the main source of uncertainty. The extrapolation procedure (linear or non-linear) according to the limited number of experimental points (rapid apparition of cellular structure) appears as the main factor influencing the discrepancy in laminar burning velocities.

Keywords: Laminar burning velocity; Spherically expanding flames; Stretch effects; Flame speed; Consumption speed

1. Introduction

Laminar burning velocity is a fundamental property in the description of combustion processes regarding reactivity, diffusivity, and

* Corresponding author. Address: Institute for Combustion Technology, RWTH Aachen University, Templergraben 64, 52056 Aachen, Germany. Fax: +49 241 80 92923.
E-mail address: emilien.varea@itv.rwth-aachen.de (E. Varea).

http://dx.doi.org/10.1016/j.proci.2014.05.137
1540-7489/

exothermicity of a combustible mixture. The laminar burning velocities is a global kinetic parameter used for validating chemical kinetic mechanisms [1,2]. Furthermore, it is one key parameter in turbulent combustion modeling, where in many combustion models turbulent flame speed depends on the laminar burning velocity. Since the demand on accurate modeling is growing, accurate measurements of this fundamental value have to be provided from experiments.

The laminar burning velocity is defined by considering a one-dimensional, stationary, adiabatic, and unstretched propagating flame. It corresponds to the velocity with which the fresh premixed gases approach the stationary flame front [3]. It is generally referred to as S_l^0, where the superscript refers to as zero stretch. This quantity is universal and only depends on the initial thermodynamic conditions (pressure and temperature) as well as the type of fuel and the composition of the premixed gases. This concept is based on the *kinematic definition*, where S_l^0 is expressed with respect to the unburned gas [4]. It can be easily shown that under these consideration, the laminar burning velocity can be written also as *consumption speed*, S_c^0, which considers the reaction rates, $\dot{w}_k$, of a species k during the reaction process [4,5]

$$S_c^0 = \frac{1}{\rho_u (Y_k^b - Y_k^u)} \int_{-\infty}^{+\infty} \dot{\omega}_k dx, \tag{1}$$

where Y_k is the mass fraction of species k, ρ_u is the unburned density, and superscripts b and u denote burned and unburned gas, respectively. This relation obviously only holds for species for which $Y^b - Y^u \neq 0$. This velocity corresponds to the mass of species k that is converted in the region between the burned and unburned zones. However, it is not possible to determine laminar burning velocities experimentally using this formulation. It represents a global quantity, directly linked to $\dot{\omega}_k$, and must be modeled, since its evolution over the flame front cannot be measured.

Considering non-stationary conditions, the flame moves in the laboratory frame of reference with a velocity that is called here the propagation speed. Hence, the difference of the propagation speed and the velocity of the fresh gases results in the laminar burning velocity [6].

Different experimental techniques have been used to measure laminar burning velocities, such as spherically expanding flames in a closed vessel [7], counterflow premixed twin-flames [8], and the heat flux burner [9]. Considering spherically expanding flames, numerous studies have been done for improving the determination of S_l^0. Stretch modifies the laminar burning velocity. However, this parameter has not been taken into account until Wu and Law in 1984 [10]. The stretch factor κ appeared as the scalar controlling the flame speed. The theory predicts a linear scaling of the stretched flame speed as $S_l = S_l^0 - \ell\kappa$, where ℓ denotes the Markstein length. With experimental data for different stretch factors, the Markstein length can be determined and an extrapolation to zero stretch can be performed. Discrepancies among different experimental data sets considerably reduced after that [11]. However, to overcome the inherent difficulty associated to small radius range available in experiments, Kelley and Law [12] and Halter et al. [7] found that a non-linear relation must be used for the extrapolation to zero stretch as for instance $[S_l/S_l^0]^2 ln[S_l/S_l^0]^2 = -2\ell\kappa/S_l^0$.[1] Recently, Kelley et al. [13] improved the non-linear relation by relaxing the quasi-steady state behavior. This reduced extrapolation errors on the Markstein length, but extrapolations of the flame speed showed no significant improvement. Chen [14] showed with an analysis of data from 1D simulations of spherically expanding flames that depending of the Lewis number Le of the mixture, the non-linear formulation of Kelley and Law [12] or Frankel and Sivashinsky [15] give the best results. He found that Sivashinsky's formulation is the most accurate for mixtures with large Lewis numbers, while at small Lewis numbers, Kelley's should be used. In addition to the extensive work on extrapolation techniques, the formulation used for determining the flame speed S_l from the observed flame dynamics should also be reconsidered. Indeed, different assumptions in the typically used formulations might lead to possible sources of uncertainty.

In the past, Fiock and Marvin [16], Linnett [17], Andrew and Bradley [3], and more recently Varea et al. [18,19] and Bonhomme et al. [20], have provided and improved different formulations to provide more reliable ways to extract information on burning velocities from spherically expanding flames.

In this work, two formulations for laminar burning velocities are investigated, namely $S_{l,d}^0$ and $S_{l,i}^0$, where d and i subscripts refer to as the direct and indirect measurement methods, see Sections 2.1 and 2.2, respectively. It focuses on the case of a lean hydrogen/air flame (Le < 1). Figure 1 compares the unstretched laminar burning velocities (from [21–24] over a range of equivalence ratios ϕ from 0.40 to 0.75. Burning velocities differ up to 20 cm/s. For the identical experimental setup, the two formulae, here called $S_{l,d}^0$ and $S_{l,i}^0$, show differences up to 10 cm/s. Therefore, in this work we:

- Identify and discuss the assumptions involved in the formulations that are commonly used for laminar burning velocity determination.

[1] In Kelley and Law [12] and Halter et al. [7], the non-linear formulation was used on the propagation speed S_f, the time derivative of the flame radius, and not directly on S_l. See 2.2 for further explanations.

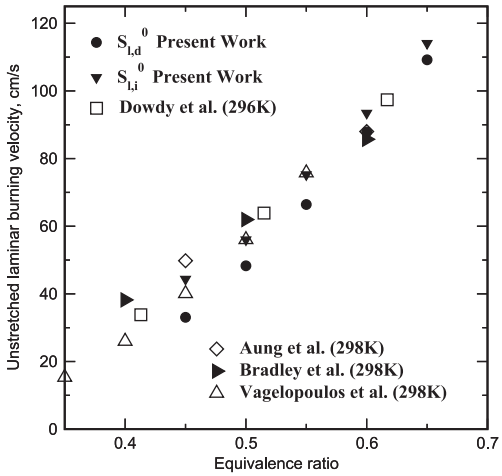

Fig. 1. Comparison with literature of unstretched indirect flame speeds (non-linearly extrapolated) $S_{l,i}^0$ and direct flame speeds $S_{l,d}^0$ for hydrogen/air flames, $p = 0.1$ MPa. Vagelopoulos et al. [21], Dowdy et al. [22], Aung et al. [23], Bradley et al. [24].

- Compare the stretched and unstretched velocities extracted from the experiments (Tomography and Schlieren) for lean hydrogen air flame at $\phi = 0.50$.
- Extend the analysis by numerical simulations of spherical 1D flames.

2. Flame speed formulations

One commonly used way to measure laminar burning velocities observes spherically expanding flames in constant volume combustion vessels. Different ways to extract the unstretched laminar burning velocities from this experiment have been proposed and used in the literature. Here, two different formulations for flame speeds are discussed, the direct and indirect formulations, $S_{l,d}$ and $S_{l,i}$, respectively.

2.1. Direct formulation for laminar flame speed, $S_{l,d}$

A propagating expanding spherical flame develops from the ignition point into the fresh gases and can be recorded, for instance, by a tomographic or a Schlieren optical diagnostic method. The time rate of change of R_f is measured in the laboratory frame. The time derivative of the radius provides the propagation speed S_f as $S_f = dR_f/dt$. Considering a chamber with a large radius, it was found that there is a quasi-steady state stage, where the flame is almost not affected by the ignition energy, such as in the early stage, or by pressure rise, as in the later stage. In this view, pressure and temperature rise due to compression are null and the flame is affected only by stretch caused by strain and curvature. When the observer is positioned on the flame, it is possible to evaluate the velocity at which fresh gases pass through the flame. It corresponds in the laboratory frame of reference to the difference of the propagation speed and the velocity of the fresh gases in that frame of reference, U_g. This is called here direct flame speed and is evaluated as

$$S_{l,d} = S_f - U_g. \tag{2}$$

For their review, Andrews and Bradley [3] used hot wire anemometry to measure the fresh gas velocity. Nonetheless, measurements of the direct flame speed have rarely been done, because of the inherent difficulty in the experimental determination and post-processing of the flow velocity ahead of the flame. With the improvement of technology and computer-aided post-processing algorithms, it is nowadays possible to measure the fresh gas velocity profile in the first millimeters ahead of the flame front with high accuracy [18,19,25,26]. According to Groot and De Goey [27], for spherically expanding flames, heat diffusion in the preheat zone influences the fresh gas velocity, U_g, which has a maximal value at the entrance of the flame front. This is the procedure to experimentally and numerically identify the velocity U_g used in Eq. (2). Note that experimentally, S_f is measured at an isothermal of the tracer evaporation (tomography) or at a specific optical gradient index (Schlieren). Numerically, S_f is derived from radii measured at the maximum of the total heat release rate. Therefore, S_f and U_g are not measured at exactly the same position, and the physical meaning of $S_{l,d}$ is slightly different than that of the above-defined ideal quantity S_l. However, it should be noted that this difference goes away for infinitely large radius, which corresponds to zero stretch.

2.2. Indirect formulation for laminar flame speed and consumption speed

An alternative method to determine the laminar burning velocity is by only using the propagation speed in combination with the jump condition across the flame. As the propagation speed is associated to the burned side, formulating the jump conditions across the flame for evaluating the flame speed, S_l, which is associated to the fresh side, results in the following assumptions:

- The burned gas is motionless, $U_b = 0$.
- The flame thickness is small compared to the flame radius.
- The burned gas density is constant and equal to the equilibrium value.

Then, applying the jump conditions yields

$$S_{l,i} = \frac{\rho_b^{eq}}{\rho_u}\frac{dR_f}{dt} \tag{3}$$

This leads to the following used formulation for laminar burning velocity determination for the spherically expanding flame configuration.

For their work, Bonhomme et al. [20] expressed a consumption speed with respect to a product species, S_c^p. They derived Eq. (1) for spherical coordinates [5] and found

$$S_c^p = \frac{\overline{\rho_b}}{\rho_u}\frac{dR_f}{dt} + \frac{R_f}{3\rho_u}\frac{d\overline{\rho_b}}{dt}, \tag{4}$$

where $\overline{\rho_b}$ is the burnt gas density (spatially averaged) and R_f is identified as a flame radius based on the mass of products. The calculation is done knowing the total mass of products and the spatially averaged product density, see reference [20] for further details. From Eq. (4), assuming that the burned gas density is constant and equal to the equilibrium value, the indirect flame speed $S_{l,i}$ is recovered. Assuming an isentropic compression for the fresh gases, Bonhomme et al. [20] also derived Eq. (1) for the fuel, S_c^f, yielding

$$S_c^f = \frac{dR_f}{dt} - \frac{R_0^3 - R_f^3}{3R_f^2}\frac{1}{\gamma_u p}\frac{dp}{dt}, \tag{5}$$

where γ_u is the ratio of the heat capacities in the fresh gases, p the pressure and R_f is the flame radius based on the fuel mass. In Eq. (5), the pressure trace and its derivative are needed during the time before the pressure increase impacts the reaction kinetics. Experimentally, this measurement is quite challenging. Therefore, this formula is not used in the experiments described below.

One can see that from these developments, the flame speed can be extracted from the direct flame speed, $S_{l,d}$, by an evaluation of the velocity field ahead of the flame front combined with the propagation speed. Flame speed is directly measured. Using the indirect formulation, important assumptions are involved on the thermodynamic state of the burned gases. In both cases, extrapolation procedures to zero stretch are needed, and one can ask whether $S_{l,d}^0$ and $S_{l,i}^0$ are equal. Previous studies reported the lack of accuracy of the indirect method [18–20,25,28]. Recently, Jayachandran et al. [29] showed that for flames subjected to radiation processes, the direct method remains the only valid formula.

2.3. Connection between the direct and indirect flame speed

One remaining question should concern the way the two formulations, $S_{l,d}$ and $S_{l,i}$ are connected. Assuming jump conditions and burned gases at equilibrium, Poinsot and Veynante [5] expressed the velocity of fresh gases ahead of the flame front as:

$$U_g = \begin{cases} 0 & \text{if } 0 < r < R_f \\ \left(\frac{R_f}{r}\right)^2\left(1 - \frac{\rho_b^{eq}}{\rho_u}\right)\frac{dR_f}{dt} & \text{otherwise} \end{cases} \tag{6}$$

Then, combining Eqs. (2) and (6) calculated at $r = R_f$, the indirect flame speed formulation, $S_{l,i}$, is retrieved. This shows the coherence between the two formulations and also highlights the degree of assumptions involved in the indirect flame speed formulation.

3. Experimental setup and numerical simulation

In this section the experimental spherical vessels for the flame speed measurements are briefly described. Hereafter, the setups are refereed to as CORIA and ITV, as they refer to as the laboratories' names where the experiments were performed. Details on the numerical simulations performed with the A-SURF code are also presented.

3.1. Experimental setup

The CORIA's apparatus is described in [18,26]. The principal difficulty in extracting the direct flame speed (Eq. (2)) lies with the accuracy of the fresh gas velocity measurement near the preheat zone of the flame front [27]. The algorithm has been detailed and validated in [18,19,26].

Experimental propagation speeds ($S_f = \frac{dR_f}{dt}$) also are extracted from Schlieren recordings performed at ITV. The experimental setup is described in detail in [30]. Since lean hydrogen air flames are known for becoming quickly cellular while expanding, the Schlieren technique can provide useful information concerning the global wrinkling of the flame shape.

3.2. Numerical simulation

A-SURF [31,32], is used to simulate the one-dimensional outwardly propagating spherical flames. Details on the governing equations, numerical schemes and code validation of A-SURF can be found in [31,32]. The spherically expanding flame is initiated by a hot pocket of burned product surrounded by fresh mixture at 300 K. The size of the hot pocket is chosen to minimize the effects of ignition, according to [31,33]. The initial wall temperature, pressure and velocity at each grip point prior to ignition are 300 K, 1 atm and 0 cm/s, respectively. The chamber radius is 50 cm large. The detailed hydrogen mechanism of Burke et al. [34] is used. The chemical reaction rates as well as thermodynamic and transport properties are evaluated using the

CHEMKIN and TRANSPORT packages [35] interfaced with A-SURF. To assess the radiation effects, two models are used, the adiabatic model (ADI) and the optically thin model (OTM) that includes the radiation emission from H_2O, CH_4, CO, and CO_2 [36].

The experiments as well as the simulation are performed in constant volume chambers. However, for small radius range, less than a third of the chamber radius, confinement effects are negligible and the flame propagates at constant pressure [33,37]. Consequently, one can conclude that the flame is only affected by stretch.

4. Results and discussion

Lean hydrogen air flames are chosen, since a large scatter of data is observed in the literature as shown in Fig. 1. To improve the quality of propagation speed measurement, a low ratio of flame velocity and recording sampling rate (limited at 5 kHz for high speed PIV) is desired. This is improved at low equivalence ratio, which, however, can also lead to the occurrence of cellular flames. To optimize this tradeoff, equivalence ratios in a range of $\phi = 0.45 - 0.65$ are studied here. However, the detailed analysis will be presented here only for $\phi = 0.50$.

4.1. Comparison of flame speed from tomography and Schlieren techniques

Figure 2 shows sequences from tomography and Schlieren techniques for the H_2/air flame at $\phi = 0.50$ and $T = 300$ K. From the Schlieren images, the flame shape starts being cellular at around 3 ms, when it starts at around 5 ms from the tomography images. This difference may affect the raw data of the propagation speed, since cellular patterns make the flame burn faster. This phenomenon is depicted in Fig. 2(i), where both stretched propagation speeds from tomography and Schlieren show a plateau for stretch below 450 s^{-1}. The corresponding maximum radius assumed to be free of cellular patterns is close to 14 mm corresponding to a time of 4 ms.

4.2. Comparison of experimental and numerical data

The case of $\phi = 0.50$ was also numerically investigated. Figure 3 shows the results comparing experimental data from the two setups (CORIA and ITV) and simulations. From Fig. 3, we observe that the propagation speed from simulation is reproducing the experiments quite well. The fresh gas velocity from the simulation and from experiments are also in a good agreement. As a result, the simulation can be used for further analysis, since both flow dynamics and flame stretch dynamics are well reproduced.

In Fig. 1 for $\phi = 0.50$, we observe that the nonlinearly extrapolated value of the indirect flame speed $S_{l,i}$ yields a higher value than that obtained as the direct flame speed, $S_{l,d}$. In previous studies,

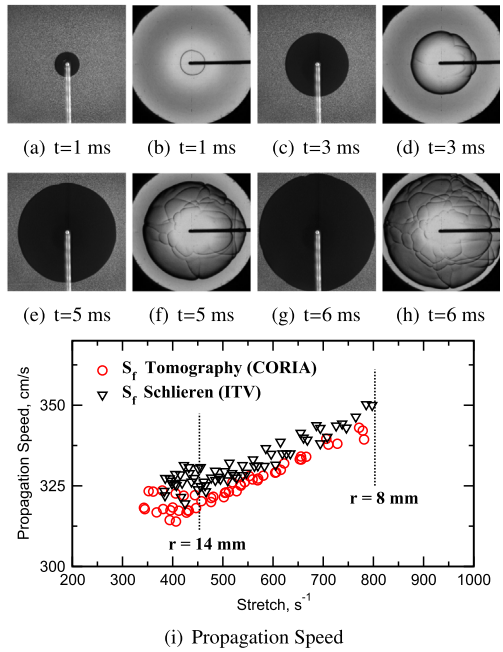

Fig. 2. Visualization sequence (tomography and Schlieren) of a hydrogen/air flame at $\phi = 0.50$, $p = 0.1$ MPa, $T = 300$ K, and corresponding propagation speeds S_f.

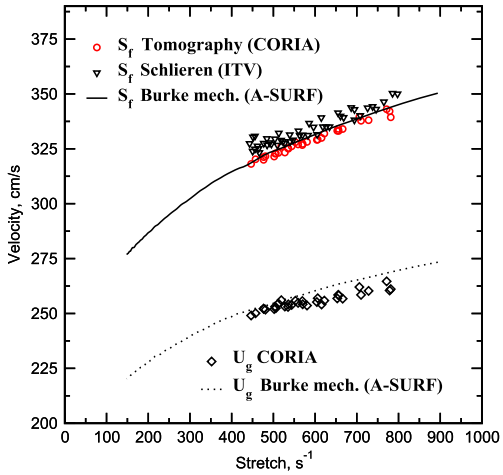

Fig. 3. Comparison of stretched velocities obtained from experiments and simulation as mentioned. Simulations are using radiative model (OTM). H_2/air flame at $\phi = 0.50$, $p = 0.1$ MPa, $T = 300$ K.

Varea et al. [18] demonstrated that in case of methane/air flames, where the Lewis number is close to unity, no differences are observed between the indirect an the direct flame speed formulations. However, for propane/air flames (Le > 1), Balusamy et al. [25] pointed out differences between both methodologies. That study attributed these differences to the confinement effect, which tends to reduce the propagation speed. Nevertheless, according to the Schlieren recordings, the maximum radius used is only 14 mm corresponding to 16% of the inner radius, which is much less than the 30%, as recommended in [33,37], where it was found that the chamber confinement effects start disturbing the flame. Then, the differences between both methodologies cannot only be explained by confinement effects.

In the next section, essential parameters that could explain the differences observed between the measured values of $S_{l,i}$ and $S_{l,d}$ are investigated.

5. Parameters influencing the stretched flame speeds and unstretched laminar burning velocities

This section focuses on the effect of stretch, non-unity Lewis numbers as well as radiative processes and extrapolation procedures. These parameters could be potential sources of errors in the estimation of the stretched flame speeds and unstretched laminar burning velocities.

5.1. Radiation processes

As mentioned above, $S_{l,i}$ cannot be determined without burned gas density, which is always assumed to be at equilibrium condition. Radiative losses may have an impact on the burnt gas density. Radiation would imply the burned gas temperature to be lower than the adiabatic flame temperature, even for the unstretched flames. As shown in Chen [32], a back flow in the burned side is generated. This is highlighted by a non-zero value of the term $\frac{R_f}{3\rho_u}\frac{d\rho_b}{dt}$ in Eq. (4) that would lower the indirect flame speed. This point was also found from asymptotic studies in [38]. Santner et al. [38] provided a solver to estimate the error induced by radiation processes. The impact of the back flow using their numerical tool is supposed to be lower than 0.5% on S_l^0. For the present case, simulations were performed for the adiabatic case and the non-adiabatic case considering a thin, gray gas approximation for radiative heat losses. No differences were observed for the velocity profiles as well as for the temperature profiles. Presentation of the results is therefore omitted.

5.2. Stretch and Lewis number effects

For a stretched flame, differential thermal/mass diffusivity can affect the flame's properties and dynamics. Thermodynamic conditions of the gases within the flame and on the burned side [20,39] differ from a planar flame. In stretched flames, the equilibrium state is not satisfied, since the flame's temperature is affected by stretch as shown by Clavin and Williams [40], Matalon and Matkowsky [41], and Law et al. [42]. Assuming that ρ_b does not vary in space and flames are subjected to small stretch, the burned gas flame temperature can, from the theory, be expressed as

$$\frac{T_b - T_{ad}}{T_{ad}} = \left(\frac{1}{Le} - 1\right)\frac{D}{\left(S_l^0\right)^2}\kappa, \tag{7}$$

where D is the thermal diffusivity of the mixture.

This equation clearly shows that stretch and non-unity Lewis numbers deviate flame temperatures from the adiabatic value. The aforementioned deviation in flame temperature directly modifies burned gas density. For Lewis numbers lower than unity, as for instance hydrogen at $\phi = 0.50$ with Le ≈ 0.51, the burned gas temperature reaches a super-adiabatic value such that $T_b > T_{ad}$, as shown in the top panel in Fig. 4. As a consequence of the super-adiabatic flame temperature, the density takes lower values. The combination of stretch and non-unity Lewis number creates a focusing effect of the reactant species H_2. The fuel H_2 diffuses into the stretched flame faster than O_2, changing the equivalence ratio at the position of the flame. As shown in Fig. 4, the fresh gases are exactly at $\phi = 0.50$, whereas the equivalence ratio on the burned side is close to $\phi = 0.58$. The temperature on the burnt side is consequently shifted to the adiabatic temperature at $\phi = 0.58$, which is $T_{ad} = 1806$ K. As a result, a correction can be applied to $S_{l,i}$ to take

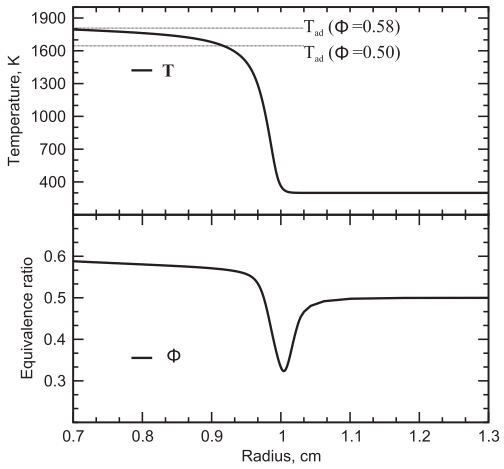

Fig. 4. Focusing effect of the reactant H_2 due to stretch and non-unity Lewis number from numerical simulation. Flame radius is positioned at $R_f = 0.98$ cm. Top: Temperature profile. Bottom: Equivalence ratio. H_2/air flame at $\phi = 0.50$, $p = 0.1$ MPa, $T = 300$ K.

into account the super-adiabatic effects, yielding $S^*_{l,i} = \rho^*_b/\rho_u S_f$, where ρ^*_b is the burned density that includes the stretch effects (Eq. (7)). Although, when stretch is null, according to Eq. (7), the adiabatic temperature is recovered so that burned gases are at equilibrium. To that point, S^0_l determined by $S_{l,i}$ or $S^*_{l,i}$ should not be different. This point is discussed hereafter.

5.3. Extrapolation models

To compare extrapolation procedures on experimental and numerical data, simulated flames are reduced to the experimental radius range ($0.8\text{ cm} < R_f < 1.4\text{ cm}$). Results are shown in Fig. 5, where extrapolation of $S_{l,d}$, $S_{l,i}$ and $S^*_{l,i}$ are considered. The determination of $S_{l,d}$ by subtracting two large quantities, S_f and U_g, may lead to scattered data. However, as in [19], the statistical error is found to be less than 5% (~2.5 cm/s). Moreover, as the mixture exhibits a Lewis number below unity, non-linear extrapolations are calculated according to Kelley and Law [12], based on investigations by Chen [32]. Since linear extrapolations of $S_{l,i}$ and $S^*_{l,i}$ are very close to the non-linear extrapolations, linear extrapolations are only reported for $S_{l,d}$.

From the experimental results, the extrapolated values of $S^0_{l,i}$ and $S^{*0}_{l,i}$ show similar unstretched velocities (<2 cm/s). As previously mentioned in Section 5.2, a misestimation of the flame's dynamic given by the indirect flame speed formula $S_{l,i}$ is shown. The real Markstein length from the indirect flame speed formulation must be corrected using the correct temperature, if the indirect flame speed dynamic is of interest. However, in agreement with the theory, Eq. (7), both formulae give the same laminar burning velocity.

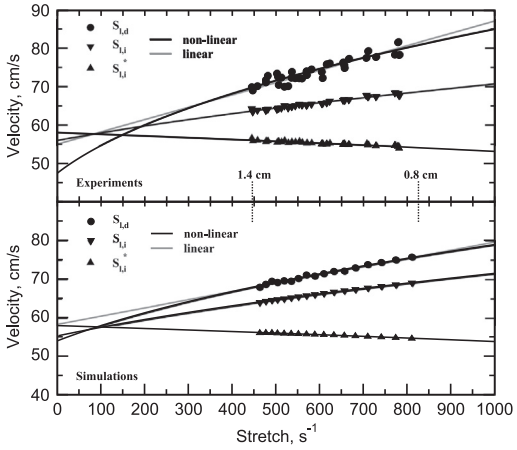

Fig. 5. Extrapolation models applied on $S_{l,d}$, $S_{l,i}$ and $S^*_{l,i}$ flame speeds. Top: Experiments. Bottom: Simulations. H_2/air flame at $\phi = 0.50$, $p = 0.1$ MPa, $T = 300$ K.

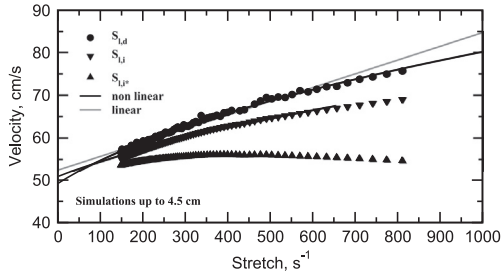

Fig. 6. Non-linear extrapolation of the full simulation. H_2/air flame at $\phi = 0.50$, $p = 0.1$ MPa, $T = 300$ K.

Nonetheless, non-linear extrapolation of $S_{l,d}$ is almost 10 cm/s below $S^0_{l,i}$ and $S^{*0}_{l,i}$.

From the simulations, we observe that $S^0_{l,d}$, $S^0_{l,i}$ and $S^{*0}_{l,i}$ are ranging from 54 to 58 cm/s. This agreement corroborates the expected behavior predicted by the theory that all formulae should lead to an identical unstretched value.

To point out the importance of the available data points for the extrapolation procedure, a full simulation for radii up to 4.5 cm was also performed. Results are shown in Fig. 6. The three velocities seem to point to a value that is close to 50 cm/s, which is 5–8 cm/s below the unstretched values extracted according to the experimental radius range. It is worth noting that even though the flame is large, this unstretched value is still away from the 1D planar flame simulation performed with the same mechanism, which is 46.74 cm/s. Hence, the remaining error results from inaccuracies of the non-linear extrapolation formula.

These results show that on the one hand, for experimental flames subjected to long ignition disturbances or to cellular patterns, the extrapolation procedure might lead to errors, on the other hand, the extrapolation formula might also lead to large errors. The reason for the latter is that these extrapolation formulations (linear or non-linear) come from asymptotic developments and are mostly valid for restricted conditions, low stretched flames and close to unity Lewis number, which are not fulfilled for lean H_2 flames.

6. Conclusion

Detailed analysis of formulations to extract stretched and unstretched burning velocities in the spherically expanding flame configuration is conducted. The direct flame speed and indirect flame speed formulations are presented, and the assumptions involved in the derivation processes are pointed out. These two flame speeds are investigated experimentally and numerically (1D propagating spherical flames) for a lean H_2/air flame ($Le < 1$), for which considerable differences

between the two formulations are observed. Therefore, the main conclusions are:

- From the experiments, cellular patterns appear for a small radius of $R_f \approx 1.4$ cm. As a consequence, the raw experimental data range is reduced to highly stretched values.
- Radiation processes have shown to be negligible and no back flow appears in the burned side is observed, which would lower the indirect flame speed.
- Stretch and non-unity Lewis numbers create a focusing effect of H_2. As a result, the local equivalence ratio within the reaction zone rises up to 16%. Consequently the burned gas temperature, and as a result the density in the burned region, differs form the adiabatic value. The response to stretch of $S_{l,i}$ is affected. However, from the simulation, both $S_{l,d}$ and $S_{l,i}$ point to a same value, which is consistent with the theory.
- Uncertainties due to the extrapolation procedure are pointed out. The full DNS (radii up to 4.5 cm) is used for the extrapolation to zero stretch. As a result, the extrapolation using only the experimental range of stretch values overestimates the extrapolated value from the full DNS range by about 10–12%. Nonetheless, the full DNS unstretched value is still 10% above the one from the 1D planar flame. This latter error only comes from the extrapolation formula, which consequently contributes to a large fraction of the error.
- Several of the errors in the actual evaluation methods, for instance the Lewis number effects, depend on stretch. That is why the stretched burning velocities are different depending on how they are evaluated, which also implies that they have different physical meaning. However, it is interesting that these stretch effect vanish when extrapolated to zero stretch.

This demonstrates that for experimental flames subjected to long ignition disturbances or to cellular patterns, the extrapolation procedure leads to errors. Further, also the extrapolation formula can lead to errors of about the same magnitude.For their recent study, Jayachandran et al. [29] mentioned as well the issue of the extrapolation procedure and the incapability of using extrapolated data to validate kinetic models. As discussed and presented in the present work, Jayachandran et al. [29] propose to compare raw experimental data from spherically expanding flames against spherical 1D flames. Therefore, uncertainty associated with extrapolation procedure is removed.

Acknowledgments

E. Varea, J. Beeckmann and H. Pitsch thank the Cluster of Excellence "Tailor-Made Fuels from Biomass", which is funded by the Excellence Initiative of the German federal state governments to promote science and research at German universities. Z. Chen thanks the support from National Natural Science Foundation of China (Nos. 51322602 and 51136005). B. Renou thanks the European Regional Development Fund under Grant Interreg IV E3C3.

References

[1] C.K. Law, C.J. Sung, H. Wang, *AIAA J.* 41 (2003) 1629–1646.
[2] A. Holley, X. You, E. Dames, H. Wang, F.N. Egolfopoulos, *Proc. Combust. Inst.* 32 (2009) 1157–1163.
[3] G.E. Andrews, D. Bradley, *Combust. Flame* 18 (1972) 133–153.
[4] T. Poinsot, T. Echekki, M.G. Mungal, *Combust. Sci. Technol.* 81 (1992) 45–73.
[5] T. Poinsot, D. Veynante, Theoretical and Numerical Combustion, third ed., 2011. <http://www.cerfacs.fr/elearning>.
[6] N. Peters, *Turbulent Combustion*, Cambridge University Press, 2000.
[7] F. Halter, T. Tahtouh, C. Mounaïm-Rouselle, *Combust. Flame* 157 (2010) 1825–1832.
[8] Y. Huang, C.J. Sung, J.A. Eng, *Combust. Flame* 139 (2004) 239–251.
[9] K.J. Bosschaart, L.P.H. De Goey, *Combust. Flame* 136 (2004) 261–269.
[10] C.K. Wu, C.K. Law, *Proc. Combust. Inst.* 20 (1984) 1941–1949.
[11] C.K. Law, *Proc. Combust. Inst.* 31 (2007) 1–29.
[12] A.P. Kelley, C.K. Law, *Combust. Flame* 156 (2009) 1844–1851.
[13] A.P. Kelley, J.K. Bechtold, C. Law, *J. Fluid Mech.* 691 (2012) 26–51.
[14] Z. Chen, *Combust. Flame* 158 (2011) 291–300.
[15] M.L. Frankel, G.I. Sivashinsky, *Combust. Sci. Technol.* 31 (1983) 131–138.
[16] E.F. Fiock, C.F. Marvin, *Chem. Rev.* 21 (1937) 367–387.
[17] J.W. Linnett, Six Lectures on the Basic Combustion Process. Detroit, Michigan: ETHYL Corporation, 1954, 1–37.
[18] E. Varea, V. Modica, A. Vandel, B. Renou, *Combust. Flame* 159 (2012) 577–590.
[19] E. Varea, V. Modica, B. Renou, A. Boukhalfa, *Proc. Combust. Inst.* 34 (2012) 735–744.
[20] A. Bonhomme, L. Selle, T. Poinsot, *Combust. Flame* 160 (2013) 1208–1214.
[21] C.M. Vagelopoulos, F.N. Egolfopoulos, C.K. Law, *Proc. Combust. Inst.* 25 (1994) 1341–1347.
[22] D.R. Dowdy, D.B. Smith, S.C. Taylor, A. Williams, *Proc. Combust. Inst.* 23 (1990) 325–332.
[23] K.T. Aung, M.I. Hassan, G.M. Faeth, *Combust. Flame* 112 (1998) 1–15.
[24] D. Bradley, M. Lawes, K. Liu, S. Verhelst, R. Woolley, *Combust. Flame* 149 (2007) 162–172.
[25] S. Balusamy, A. Cessou, B. Lecordier, *Exp. Fluids* 50 (2011) 1109–1121.
[26] E. Varea, PhD Thesis. <http://tel.archives-ouvertes.fr/tel-00800616>.
[27] G.R.A. Groot, L.P.H. De Goey, *Proc. Combust. Inst.* 29 (2002) 1445–1451.

[28] Z. Chen, M.P. Burke, Y. Ju, *Combust. Theory Model.* 13 (2009) 343–364.
[29] J. Jayachandran, R. Zhao, F.N. Egolfopoulos, Combust. Flame (in press). http://dx.doi.org/10.016/j.combustflame.2014.03.009
[30] J. Beeckmann, L. Cai, H. Pitsch, *Fuel* 117 (Part A) (2014) 340–350.
[31] Z. Chen, M.P. Burke, Y. Ju, *Proc. Combust. Inst.* 32 (2009) 1253–1260.
[32] Z. Chen, *Combust. Flame* 157 (2010) 2267–2276.
[33] D. Bradley, P.H. Gaskell, X.J. Gu, *Combust. Flame* 104 (1996) 176–198.
[34] M.P. Burke, M. Chaos, F.L. Dryer, S.J. Klippenstein, *Int. J. Chem. Kinet.* 44 (2012) 444–474.
[35] R.J. Kee, J.F. Grcar, M.D. Smooke, J.A. Miller, Sandia National Laboratory Report SAND85-8240.
[36] Z. Chen, X. Qin, B. Xu, Y.G. Ju, F.S. Liu, *Proc. Combust. Inst.* 31 (2007) 2693–2700.
[37] M.P. Burke, Z. Chen, Y. Ju, F. Dryer, *Combust. Flame* 156 (2009) 771–779.
[38] J. Santner, F.M. Haas, Y. Ju, F.L. Dryer, *Combust. Flame* 161 (2014) 147–153.
[39] J.H. Chen, H.G. Im, *Proc. Comb. Inst.* 28 (2000) 211–218.
[40] P. Clavin, F.A. Williams, *J. Fluid Mech.* 116 (1982) 251–282.
[41] M. Matkowsky, B.J. Matalon, *J. Fluid Mech.* 124 (1982) 239–259.
[42] C.K. Law, P. Cho, M. Mizomoto, H. Yoshida, *Proc. Combust. Inst.* 21 (1988) 1803–1809.